

# SCIENTIFIC REPORTS



OPEN

## Magnesium diboride coated bulk niobium: a new approach to higher acceleration gradient

Teng Tan<sup>1,†</sup>, M. A. Wolak<sup>1</sup>, X. X. Xi<sup>1</sup>, T. Tajima<sup>2</sup> & L. Civale<sup>2</sup>

Received: 26 April 2016

Accepted: 07 October 2016

Published: 24 October 2016

Bulk niobium Superconducting Radio-Frequency cavities are a leading accelerator technology. Their performance is limited by the cavity loss and maximum acceleration gradient, which are negatively affected by vortex penetration into the superconductor when the peak magnetic field at the cavity wall surface exceeds the vortex penetration field ( $H_{vp}$ ). It has been proposed that coating the inner wall of an SRF cavity with superconducting thin films increases  $H_{vp}$ . In this work, we utilized Nb ellipsoid to simulate an inverse SRF cavity and investigate the effect of coating it with magnesium diboride layer on the vortex penetration field. A significant enhancement of  $H_{vp}$  was observed. At 2.8 K,  $H_{vp}$  increased from 2100 Oe for an uncoated Nb ellipsoid to 2700 Oe for a Nb ellipsoid coated with ~200 nm thick  $MgB_2$  thin film. This finding creates a new route towards achieving higher acceleration gradient in SRF cavity accelerator beyond the theoretical limit of bulk Nb.

Particle accelerators are our main window to explore particle physics and understand the early universe. Bulk niobium superconducting radio frequency (SRF) cavities are the leading accelerator technology, and in the last 2 decades, their performance has been improved to being very close to the theoretical limit. New materials and/or approaches are needed to further improve the performance and reduce the cost of SRF cavities<sup>1,2</sup>. In this work, we studied the magnesium diboride ( $MgB_2$ ) coated bulk niobium and showed the coated SRF cavities have the potential to reach 30% higher acceleration gradient than the state of the art Nb cavities.

The technology of SRF cavities is based on the Meissner effect, characterized by the expulsion of magnetic field from a bulk superconducting material. In type II superconductors, such as Nb, the Meissner state can only be sustained up to a certain magnetic field, above which flux will penetrate the material in the form of vortices. In the presence of an RF excitation these vortices will oscillate, producing dissipation that drastically reduces the quality factor ( $Q$ ), thus rendering the cavity useless. The limiting factor is the maximum accelerating gradient ( $E_{acc}$ ), which is related to the maximum magnetic field parallel to the cavity surface that can be sustained without vortex penetration ( $H_{vp}$ ). In thermodynamic equilibrium,  $H_{vp}$  of a bulk superconductor in the absence of demagnetizing effects is equal to the lower critical field ( $H_{c1}$ ). However, surface barriers may preclude the vortex entry, allowing the Meissner state be retained under metastable conditions up to a higher superheating field  $H_{sh}$ <sup>3</sup>. The best Nb cavities have  $E_{acc}$  50 MV/m at temperature  $T \sim 2$  K (the operating temperature of the SRF cavities at  $f > 500$  MHz), corresponding to  $H_{vp,Nb} \sim 2000$  Oe<sup>4</sup>, which is very close to the ideal limit set by the intrinsic material properties,  $H_{sh,Nb}(2\text{ K}) \approx 2280$  Oe<sup>5</sup>.

To increase  $H_{vp}$ , Gurevich proposed coating the inside of Nb cavities with multilayers of thin superconducting films separated by insulating layers<sup>2</sup>. The idea is that the superconducting films will partially screen the cavity magnetic field, reducing it to a value lower than  $H_{vp,Nb}$  at the internal surface of the Nb wall. We will focus on the simplest case of a SRF cavity coated with a single layer of superconductor, because this S-I-S structure already exhibits all the relevant physics and detailed theoretical analyses of its shielding effect have recently been performed with various approaches<sup>6–9</sup>.

The principle of operation of the S-I-S structure involves two concepts. First, when the thickness of the superconducting film ( $d_s$ ) is comparable to or smaller than the penetration depth ( $\lambda$ ),  $H_{c1}$  for field parallel to the surface increases. This is because the internal field is nonzero everywhere within the thin film, thus the free energy cost of shielding the external field by a screening current is lowered and vortex penetration does not become

<sup>1</sup>Department of Physics, Temple University, Philadelphia, 19122, Pennsylvania, USA. <sup>2</sup>Los Alamos National Laboratory, Los Alamos, 87545, New Mexico, USA. <sup>†</sup>Present address: Institute of Modern Physics, Chinese Academy of Science, Lanzhou, China, 730000. Correspondence and requests for materials should be addressed to L.C. (email: lcivale@lanl.gov)

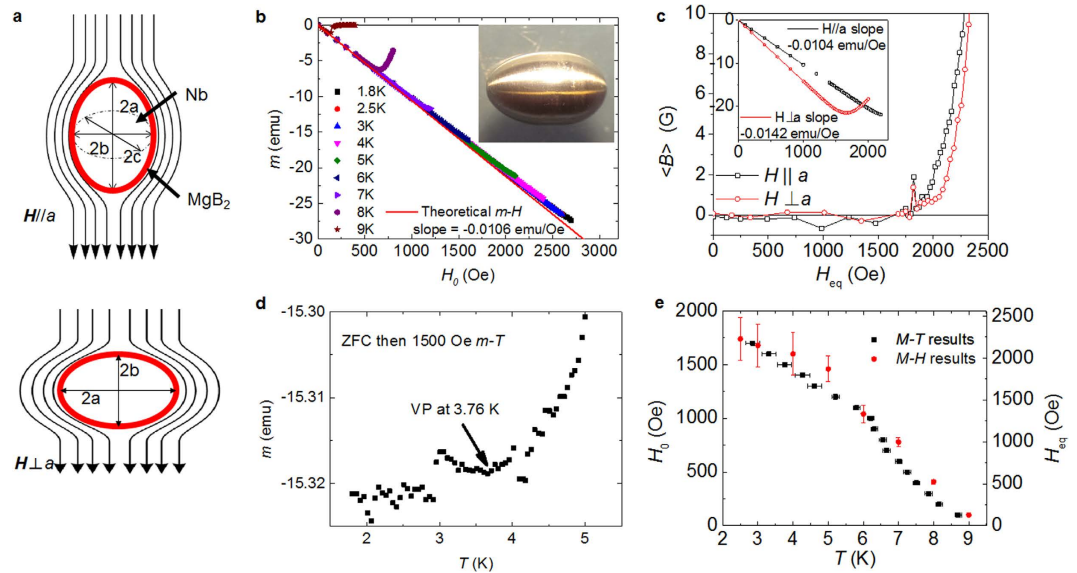


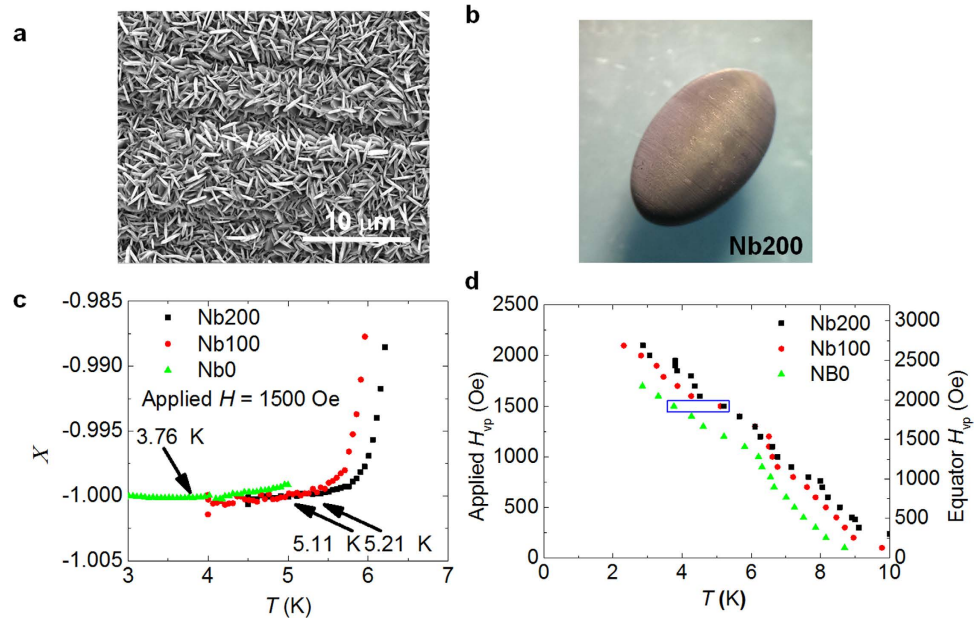
**Figure 1.** (a) Schematic of the vortex penetration field measurement. (b) ZFC  $m$ - $H$  curves of bare Nb ellipsoid at different temperatures. (c)  $\langle B \rangle$ - $H$  curves of bare Nb ellipsoid at different orientations. (d) Typical ZFC  $m$ - $T$  curve of bare Nb ellipsoid under 1000 Oe applied field. Arrow signals the temperature where  $H_{vp}$  equals the applied field. (e) Comparison of  $H_{vp}$  obtained from both methods.

favorable until a higher field. For instance, if  $H$  is applied on both sides of a film with  $d_s \ll \lambda$ ,  $H_{c1}$  increases from the bulk values  $H_{c1} \propto \Phi_0/\lambda^2$  to  $H_{c1} \propto \Phi_0/d_s^2$  (here  $\Phi_0 = 2.07 \times 10^{-7}$  Gcm<sup>2</sup> is the flux quantum). The situation is somewhat different when the field is only applied on one side<sup>6</sup>, but also in this case  $H_{c1}$  for a thin film is substantially enhanced, resulting in a higher  $H_{vp}$  for the film-coated Nb cavity<sup>10</sup>. The second concept is that the screening (reduction) of the field produced by the film is  $\Delta H \sim d_s J$ , where the superconducting current density ( $J$ ) depends on the details of the geometry but cannot exceed the superconducting depairing current density ( $J_d$ ) in the film,  $J_d \sim H_c/\lambda$ , where  $H_c$  is the thermodynamic critical field ( $H_c > H_{c1}$  in type II superconductors). It is clear from the previous considerations that if  $d_s$  is too large there is not enough  $H_{c1}$  enhancement and if it is too small  $H_{vp}$  is only increased by a small amount  $\Delta H$ , so there must be some optimum  $d_s$  that produces the largest  $H_{vp}$ . T. Kubo<sup>9,11</sup> has shown that, when the simple estimate of an exponential decay of the magnetic field from the film surface is replaced by the simultaneous solution of the Maxwell and London equations in the complete S-I-S structure with the appropriate boundary conditions,  $H_{vp}$  depends on the properties of both the coating layer and bulk superconducting materials, on  $d_s$ , and on the thickness of the insulating layer ( $d_i$ ). In particular, these studies show that the shielding effect still exists for  $d_i = 0$ , that is, without an insulating layer between the thin film and the niobium underneath. In this paper we provide the first experimental demonstration of the concept, by showing that a Nb SRF cavity coated with a single MgB<sub>2</sub> layer could sustain a higher  $H_{vp}$ , above the theoretical limit given by the  $H_{sh}$  for Nb. This could lead to SRF cavities with higher accelerating gradients.

The increase of  $H_{c1}$  in thin films for  $H$ //surface is a well-established and well understood effect<sup>10</sup>, and can be readily observed using a SQUID magnetometer. As  $H$  is increased from 0 at a fixed temperature, the initial Meissner state is characterized by a linear  $m(H)$  dependence  $m_M = -(V_{eff}/4\pi)H$ . Here  $V_{eff}$  is the effective superconductor volume, which is smaller than the geometrical volume  $V$  due to the field penetration near the surfaces. At  $H_{c1}$ ,  $m(H)$  deviates from the linear dependence, signaling vortex penetration. The  $H_{c1}$  enhancement in thin MgB<sub>2</sub> films has been studied previously using this technique<sup>12</sup>.  $V_{eff}$  for  $\delta \ll \lambda$  is very small, thus the experimental resolution of the magnetometers is a serious limiting factor for these measurements.

However the second concept of Gurevich proposal, namely that a thin film can sustain a  $\Delta H$  between both of its surfaces, cannot be tested using the approach described above because both surfaces of the film are exposed to the same ambient field. In this paper we propose a novel approach that overcomes this fundamental limitation, and concomitantly also solves the resolution and alignment problems (see supplementary information). We have fabricated macroscopic-sized ellipsoids and coated them with MgB<sub>2</sub> films. The Meissner effect in the film screens the entire ellipsoid volume from the applied field, so a  $\Delta H$  develops between the internal and external film surfaces. Here the field is outside of the ellipsoid rather than inside as in a real SRF cavity, thus we call it the “inverse cavity” concept. We use ellipsoids because the demagnetizing effects and boundary conditions are well defined, and in the Meissner state the external field at the ellipsoid surface is parallel to the surface everywhere, the same as in real SRF cavities.

The Nb ellipsoids have the nominal semi axes  $a = 4$  mm,  $b = c = 2.5$  mm, made from the same bulk material as presently used in SRF cavities. The measurements were performed in a Quantum Design MPMS SQUID magnetometer. When the applied field  $H$  is parallel to the  $i$  axis ( $i = a, b, c$ ) the calculated “Meissner slope” is  $m_{M,i}/H = -V/[4\pi(1 - N_i)] = -ab^2/[3(1 - N_i)]$ , where  $N_i$  are the demagnetizing factors, such that  $N_a < N_b = N_c$  and  $N_a + N_b + N_c = 1$ .



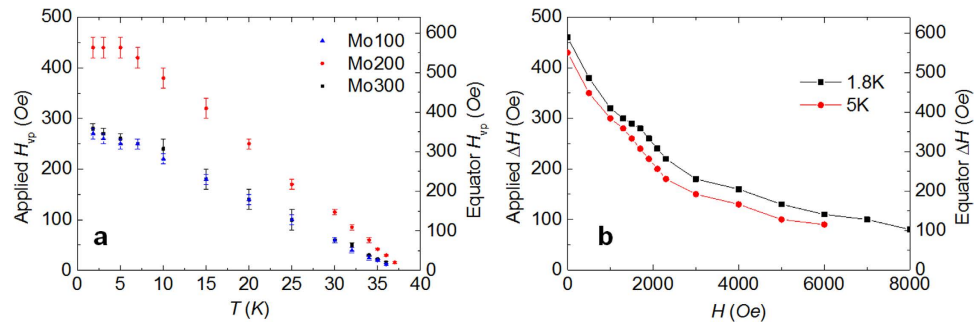
**Figure 2.** (a) SEM image taken on the Nb100 ellipsoid. (b) optical image of Nb200 ellipsoid (c)  $m$ - $T$  curves comparisons between Nb ellipsoids with different thicknesses of  $\text{MgB}_2$  coating. ZFC to 1.8 K then apply 1500 Oe field. Arrows indicate the  $H_{vp}$  of each sample. (d) Comparison of  $H_{vp}$ - $T$  curves measured on Nb ellipsoids. Data points in the blue box corresponds to the 3 curves in Fig. 2(c). The actual  $H$  field at the ellipsoids equator is calculated on the right y-axis.

Figure 1a shows the schematic of the  $H_{vp}$  measurement. Most results in this paper were measured with the applied magnetic field parallel to the long axis of the ellipsoid (top). However, the field alignment to the short axis (bottom) was also measured to confirm the results taking into account the different demagnetizing factors for the two field directions. Figure 1b presents  $m$  vs.  $H$  at several temperatures for a bare Nb ellipsoid shown in the inset. For each  $T$ , the sample was cooled from above  $T_c = 9.3$  K to  $T$  in  $H = 0$  (zero field cooling, ZFC) before the  $m$  vs.  $H$  measurement. The Meissner slope does not change with  $T$  because the variation of the effective superconductor volume due to the change in  $\lambda(T)$  is too small compared to the dimensions of the ellipsoid. The solid line in this figure corresponds to the predicted  $m$ - $H$  relationship for the ellipsoid with  $a = 4$  mm and  $b = c = 2.5$  mm in the Meissner state. The  $m$  vs.  $H$  curves at  $T = 5$  K for the Nb ellipsoid are shown in the inset of Fig. 1c for both  $\mathbf{H} \parallel a$  and  $\mathbf{H} \perp a$ . From the slopes of both orientations  $m_{M,a}/H$  and  $m_{M,b}/H$ , we obtained  $N_a = 0.1880$  and  $N_b = N_c = 0.4060$ . The ellipsoid volume was calculated to be  $V = 0.1062$  cm<sup>3</sup>, in excellent agreement with the designed value (from the weight of this particular ellipsoid we had determined  $V = 0.1048$  cm<sup>3</sup>).

Although the applied field is uniform, due to the demagnetizing effects the total external field is not. In the Meissner state the total external field at the surface of the ellipsoid is parallel to the surface everywhere, and its magnitude varies along the surface, being zero at the poles and reaching a maximum at equator  $H_{eq} = H/(1 - N_i)$ , where  $i = a, b$ . (see Fig. 1a). Consequently, vortex penetration starts at the equator. As seen in the Fig. 1c, the average magnetic induction  $\langle B_i \rangle = 4\pi(1 - N_i)(m - m_M)/V$  of the ellipsoid starts to deviate from zero at the same  $H_{eq}$  for both  $\mathbf{H} \parallel a$  and  $\mathbf{H} \parallel b$  orientations. We define the vortex penetration field  $H_{vp}$  as when  $\langle B \rangle$  increases above the noise. The noise level increases with  $H$ , reaching about  $\pm 2$  G at 1.5 kG, which negatively impact the accuracy of the  $H_{vp}(T)$  measurement<sup>13</sup>. This high noise level could be originated from the superconducting magnet in the magnetometer when it was charged between 1000 and 5000 Oe with fine steps<sup>14</sup>.

An alternative approach to measure  $H_{vp}$  is to apply a field  $H < H_{vp}(T)$  after ZFC and then measure  $m(T)$ . A result is shown in Fig. 1d. As  $T$  increases,  $m$  initially remains constant at the Meissner value until the vortex penetration occurs, which is signaled by a sudden reduction of the absolute value of  $m$  when  $H = H_{vp}(T)$ . Figure 1e summarizes the  $H_{vp}(T)$  results obtained from both  $m(H)$  and  $m(T)$  measurements. The left and right vertical axes in Fig. 1e show the value of  $H$  and  $H_{eq}$  for first vortex penetration respectively. The error bars in Fig. 1e stand for the  $H_{vp}$  variation when using 5 G and 1 G  $\langle B \rangle$  criterion. The results suggest that the  $m$ - $T$  approach is a preferred method for the  $H_{vp}$  measurement. At high field, it is more accurate than the  $m$ - $H$  technique mainly due to the elimination of the flux creep effect from the superconducting magnet. At low  $H$  it is comparable to the  $m$ - $H$  technique. Therefore, the  $m$ - $T$  technique was used to measure  $H_{vp}$  of a bare Nb ellipsoid and two  $\text{MgB}_2$  thin film-coated Nb ellipsoids in this work. From Fig. 1e we find that at  $T \sim 2$  K vortex penetration starts at  $H_{eq} \sim 2200$  Oe, very close to the ideal limit  $H_{sh,Nb}(2\text{K}) \approx 2280$  Oe, confirming the high quality of the Nb used in our study.

The  $\text{MgB}_2$  thin film coating of Nb ellipsoids was performed using hybrid physical-chemical vapor deposition (HPCVD)<sup>15</sup>. Two Nb ellipsoids were coated with  $\text{MgB}_2$  layers of 100 nm (Nb100) and 200 nm (Nb200), respectively. Figure 2a shows an SEM image taken at the equator of the ellipsoid Nb100. The film is polycrystalline with grain size of  $\sim 1$   $\mu\text{m}$ . The  $\text{MgB}_2$  layer covered the entire ellipsoid uniformly without pinholes. An optical image of



**Figure 3.** (a) The dependence of  $H_{vp}$  of the MgB<sub>2</sub>/Mo samples on temperature.  $H_{vp}$ s of Mo100 and Mo300 are almost overlapped. (b) Maximum  $H$  difference shielded by a single layer of MgB<sub>2</sub> versus the field inside the MgB<sub>2</sub> shell for Mo200 at 1.8 K and 5 K.

Nb200 is presented as the inset to Fig. 2b. Figure 2c shows the  $m$ - $T$  curves for the bare Nb ellipsoid and the Nb ellipsoids coated with 100 nm and 200 nm MgB<sub>2</sub> layers for 1500 Oe applied field. The onset of vortex penetration are marked with black arrows in the figure. With an increasing temperature, vortices penetrate into the bare Nb ellipsoid at 3.76 K. This temperature increases to 5.11 K and 5.21 K for the Nb100 and Nb200 ellipsoid, respectively. By repeating the  $m$ - $T$  measurements, the temperature dependence of  $H_{vp}$  can be obtained.

Figure 2d summarizes the  $H_{vp}(T)$  curves for the bare Nb ellipsoid, Nb100, and Nb200. The three data points within the blue box correspond to the 3 curves in Fig. 2c. The  $H_{vp}(T)$  of Nb200 is about 400 Oe higher than the bare Nb ellipsoid in the temperature range from 1.8 K to the  $T_c$  of Nb. This increase is approximately constant because the properties of MgB<sub>2</sub> do not change significantly in this temperature range ( $T < T_c/4$ ). The maximum field at the equator that our inverse cavity can sustain before vortex penetration is indicated on the right vertical axis. At  $T \sim 2.8$  K it is  $\sim 2600$  Oe, about 500 Oe above the bare Nb ellipsoid.

As an additional test of our inverse cavity concept we deposited MgB<sub>2</sub> films of thickness  $d_s = 100$ ; 200 and 300 nm on non-superconducting molybdenum ellipsoids. For details of the measurements and analysis, see the supplementary material. For the three samples we measured  $m(H)$  at several  $T$  with  $\mathbf{H} \parallel \mathbf{a}$ . The Meissner slopes indicate that the full volume of the ellipsoids is screened, implying that the field at the MgB<sub>2</sub>-Mo interface is zero. At  $H_{vp}(T)$  the field at the interface becomes nonzero and spreads inside the Mo. The obtained  $H_{vp}(T)$  curves are shown in Fig. 3a. They extrapolate to zero at the  $T_c$  of the MgB<sub>2</sub> films ( $\sim 38.1$ ; 38.6 and 38.7 K respectively).

As described in detail in the Supplementary Materials, we found out that in all cases  $H_{vp}$  at the equator is lower than the prediction for the enhanced  $H_{c1}$ , and that the field penetration occurs when the screening current is large enough to eliminate the surface barrier. The fact that  $H_{vp}$  in the MgB<sub>2</sub> coated Mo ellipsoids is determined by  $J$  rather than  $H_{c1}$  is good news for cavity applications, because it implies that  $H_{vp}$  is the limit for the *difference* in field that can be sustained between both surfaces of the film, not for the *absolute value* of the field. This is fully consistent with our main experimental finding, namely that by adding an MgB<sub>2</sub> coating we have been able to increase  $H_{vp}$  by about 500 Oe on top of the already large penetration field of Nb.

We performed additional studies on the Mo200 ellipsoid to estimate how high  $H_{vp}$  could potentially be obtained. After applying a field  $H_{int}$  at a temperature above the  $T_c$  of MgB<sub>2</sub> (which penetrates homogeneously into the Mo), we cooled down to a measurement  $T$  and subsequently increased  $H$ . We observed an initial linear  $m(H)$  Meissner dependence, indicating that screening currents develop in the MgB<sub>2</sub> that shield the internal Mo volume from the external field variation. Eventually the surface barrier disappears and the field penetrates when the difference between the outside and the inside field,  $\Delta H = H - H_{int}$ , reaches a value  $\Delta H_{vp}$ , as summarized in Fig. 3b. The remarkable result is that  $\Delta H_{vp} > 0$  even for  $H_{int}$  well above the maximum operating fields of Nb cavities. This implies that the operating field of a cavity could be increased by  $\Delta H_{vp}/(1 - N_a)$  by internally coating it with this MgB<sub>2</sub> film. For instance, Fig. 3b shows that if a hypothetical cavity were able to sustain  $H_{vp} \sim 4000$  Oe, at 1.8 K, then this MgB<sub>2</sub> film would further increase that  $H_{vp}$  by  $\sim 200$  Oe.

Our results demonstrate three important facts. First, it is indeed possible to increase the  $H_{vp}$  of the Nb material used in the state-of-the-art SRF cavities by a substantial amount ( $\sim 600$  Oe) by coating it with a thin superconducting film that screens vortex penetration. Second, it is technically possible to deposit a thin MgB<sub>2</sub> film with appropriate properties for this purpose on curved bulk Nb. Third, a single layer of superconducting thin film can reduce the magnetic field felt by the bulk material under it. These three facts are enough to demonstrate that it is possible to increase the  $H_{vp}$  of existing Nb SRF cavities by  $\sim 600$  Oe. The superconducting shielding current density at the equator of Nb200 is estimated to be  $J \sim \Delta H/d \sim 10^7$  A/cm<sup>2</sup>, as compared to  $J_d \sim 10^8$  A/cm<sup>2</sup> reported for MgB<sub>2</sub> thin films<sup>16</sup>, therefore the maximum  $\Delta H$  that a MgB<sub>2</sub> thin film can shield has not been reached. Further, a superconductor/insulating multilayer coating proposed by Gurevich would achieve even higher shielding field  $\Delta H_{total}$  with MgB<sub>2</sub> films.

## Methods

**Deposition of MgB<sub>2</sub> thin film on Nb ellipsoids.** The MgB<sub>2</sub> films were deposited by Hybrid Physical-Chemical Vapor Deposition (HPCVD) technique<sup>15</sup>. The schematic of the deposition technique is presented in Extended Data Fig. 1(a). By heating magnesium pellets above melting temperature and letting magnesium vapor react with boron from the decomposition of diborane gas, this technique has produced the films with the highest quality on both single crystal and metallic substrates<sup>17,18</sup>. In this work, MgB<sub>2</sub> film was deposited at 730 °C in

40 Torr hydrogen atmosphere. The boron source was 20 sccm 5% diborane in hydrogen solution, which gave a growth rate of 55 nm/min. Each ellipsoid was coated three times with rotating 120 degree between each coating to achieve uniform coating. During the first deposition, a piece of  $5 \times 5 \text{ mm}^2$  silicon carbide (SiC) substrate is put aside of the ellipsoid as a reference for thickness calibration. The nominal thickness of  $\text{MgB}_2$  layer coated on the ellipsoid refers to the film thickness on the SiC substrate.

## References

1. Padamsee, H., Knobloch, J. & Hays, T. *RF Superconductivity for Particle Accelerators*. (eds Month, M. *et al.*) Ch. 14, 315–328 (Wiley, 1998).
2. Gurevich, A. Enhancement of rf breakdown field of superconductors by multilayer coating. *Appl Phys Lett* **88**, 012511, doi: 10.1063/1.2162264 (2006).
3. Bean, C. & Livingston, J. Surface Barrier in Type-II Superconductors. *Phys Rev Lett* **12**, 14–16, doi: 10.1103/PhysRevLett.12.14 (1964).
4. Ciovati, G. *Where Next with SRF*, Paper presented at IPAC2013, Shanghai, China p. 3124 (2013).
5. Hays, T. & Padamsee, H. *Measuring the RF Critical Field of Pb, Nb, and Nb<sub>3</sub>Sn*, Paper presented at the 1997 Workshop on RF Superconductivity, Abano Terme (Padova), Italy p. 789 (1997).
6. Hein, M. *High-Temperature-Superconductor Thin Films at Microwave Frequencies*. Ch. 3, 127–128 (Springer Berlin Heidelberg, 1999).
7. Posen, S., Transtrum, M. K., Catelani, G., Liepe, M. U. & Sethna, J. P. Shielding Superconductors with Thin Films as Applied to rf Cavities for Particle Accelerators. *Physical Review Applied* **4**, 044019 (2015).
8. Gurevich, A. Maximum screening fields of superconducting multilayer structures. *AIP Adv* **5**, 017112; doi: 10.1063/1.4905711 (2015).
9. Kubo, T. *Superconducting nano-layer coating without insulator*, Paper presented at LINAC2014, Geneva, Switzerland p.1026 (2014).
10. Abrikosov, A. A. On the Lower Critical Field of Thin Layers of Superconductors of the Second Group. *Soviet Physics JETP* **19**, 988–991 (1964).
11. Kubo, T. Multilayer coating for high gradients. *arXiv:1607.01495* (2016).
12. Tan, T. *et al.* Enhancement of lower critical field by reducing the thickness of epitaxial and polycrystalline  $\text{MgB}_2$  thin films. *APL Materials* **3**, 041101; doi: 10.1063/1.4916696 (2015).
13. Tan, T., Wolak, M. A., Xi, X. X., Tajima, T. & Civale, L. *Increase in vortex penetration field on Nb ellipsoid coated with a  $\text{MgB}_2$  thin film*, PAPER presented at SRF2015, whistler, Canada, p.512 (2015).
14. QuantumDesign. MPMS Service Note 1014-820, *Characterization of Magnet Noise in Superconducting Magnets When Charging the Magnetic Field in Unidirectional Steps*, <http://www.qdusa.com/sitedocs/appNotes/mpms/1014-823.pdf> (2001).
15. Zeng, X. H. *et al.* *In situ* epitaxial  $\text{MgB}_2$  thin films for superconducting electronics. *Nature Materials* **1**, 35–38; doi: 10.1038/nmat703 (2002).
16. Eisterer, M. Magnetic properties and critical currents of  $\text{MgB}_2$ . *Superconductor Science and Technology* **20**, R47–R73 (2007).
17. Zhuang, C. *et al.* Clean  $\text{MgB}_2$  thin films on different types single-crystal substrate fabricated by hybrid physical-chemical vapor deposition. *Supercond Sci Tech* **22**, 025002, doi: 10.1088/0953-2048/22/2/025002 (2009).
18. Zhuang, C. *et al.*  $\text{MgB}_2$  Thin Films on Metal Substrates for Superconducting RF Cavity Applications. *J. Supercond. Nov. Magn.* **26**, 1563–1568, doi: 10.1007/s10948-012-1969-3 (2013).

## Acknowledgements

The authors would like to thank Dr. Takayuki Kubo for his help in the theoretical analysis of  $\text{MgB}_2/\text{Nb}$  model. The magnetization studies at LANL were supported by the US Department of Energy, Office of Basic Energy Sciences, Division of Materials Sciences and Engineering. The sample preparation was supported by the US Department of Energy under grant No. DE-SC0011616. The scanning electron imaging was performed in the CoE-NIC facility at Temple University. The CoE-NIC is based on DoD DURIP Award N0014-12-1-0777 from the Office of Naval Research and is sponsored by the College of Engineering, Temple University.

## Author Contributions

L.C. first proposed to use coated Nb ellipsoids to study the thin film coated SRF cavities. T. Tan, M.A.W. and X.X.Xi prepared the ellipsoid samples and Figure 2a. L.C. and T. Tan performed the magnetic measurement and prepared all the other Figures of the main text, and Figures 1–3 of the SI. T. Tajima prepared Figure 4 of the SI. T. Tan wrote the first manuscript. All authors reviewed and revised the drafts and contributed to the final manuscript.

## Additional Information

**Supplementary information** accompanies this paper at <http://www.nature.com/srep>

**Competing financial interests:** The authors declare no competing financial interests.

**How to cite this article:** Tan, T. *et al.* Magnesium diboride coated bulk niobium: a new approach to higher acceleration gradient. *Sci. Rep.* **6**, 35879; doi: 10.1038/srep35879 (2016).



This work is licensed under a Creative Commons Attribution 4.0 International License. The images or other third party material in this article are included in the article's Creative Commons license, unless indicated otherwise in the credit line; if the material is not included under the Creative Commons license, users will need to obtain permission from the license holder to reproduce the material. To view a copy of this license, visit <http://creativecommons.org/licenses/by/4.0/>

© The Author(s) 2016